RSC Advances

PAPER

View Article Online
View Journal | View Issue

Cite this: *RSC Adv.*, 2021, **11**, 33260

Selective targeting of CD38 hydrolase and cyclase activity as an approach to immunostimulation†

Thomas Z. Benton,[a] Catherine M. Mills,[a] Jonathan M. Turner,[a] Megan J. Francis,[a] Dalan J. Solomon,[a] Pieter B. Burger,[a] Yuri K. Peterson,[a] Nathan G. Dolloff,[b] André S. Bachmann[c] and Patrick M. Woster *[a]

The ectoenzyme CD38 is highly expressed on the surface of mature immune cells, where they are a marker for cell activation, and also on the surface of multiple tumor cells such as multiple myeloma (MM). CD38-targeted monoclonal antibodies (MABs) such as daratumumab and isatuximab bind to CD38 and promote cancer cell death by stimulating the antitumor immune response. Although MABs are achieving unprecedented success in a percentage of cases, high rates of resistance limit their efficacy. Formation of the immunosuppressive intermediate adenosine is a major route by which this resistance is mediated. Thus there is an urgent need for small molecule agents that boost the immune response in T-cells. Importantly, CD38 is a dual-function enzyme, serving as a hydrolase and a nicotinamide adenine dinucleotide (NAD^+) cyclase, and both of these activities promote immunosuppression. We have employed virtual and physical screening to identify novel compounds that are selective for either the hydrolase or the cyclase activity of CD38, and have demonstrated that these compounds activate T cells *in vitro*. We are currently optimizing these inhibitors for use in immunotherapy. These small molecule inhibitors of the CD38-hydrolase or cyclase activity can serve as chemical probes to determine the mechanism by which CD38 promotes resistance to MAB therapy, and could become novel and effective therapeutic agents that produce immunostimulatory effects. Our studies have identified the first small molecule inhibitors of CD38 specifically for use as immunostimulants.

Received 18th August 2021
Accepted 3rd October 2021

DOI: 10.1039/d1ra06266b

rsc.li/rsc-advances

Introduction

The ectoenzyme known as cluster of differentiation 38 (CD38) has recently re-emerged as a viable target for immunotherapy. CD38 primarily exists as a 34 kDa transmembrane glycoprotein containing a small N-terminal cytosolic tail, a single pass transmembrane domain, and a large C-terminal extracellular domain.[1] CD38 is expressed on the surface of mature immune cells, and as adaptive immune cells mature and undergo phenotypic reprogramming, cell surface markers are expressed as part of phenotypic remodelling.[2,3] In both B and T cells, CD38 expression is indicative of cellular activation and serves as a receptor for lymphocyte transmigration.[3] Recent literature suggests that CD38 expression is highly contextual in that it depends on cellular location and the pathophysiological context in which it is embedded.[4]

For multiple reasons, CD38 is considered a promising target for small molecule inhibitors. Highly proliferating cells, such as T cells and many tumor cell lines, are highly dependent on nicotinamide adenine dinucleotide (NAD^+), suggesting that their activity is likely to be further enhanced by inhibition of the NADase function of CD38. Multiple research groups have targeted CD38 as an NAD boosting therapy in the context of aging, mitochondrial dysfunction, obesity, and diabetes.[4–8] Notably, some of these inhibitors increased the levels of NAD^+ *in vitro* and *in vivo*, but were reportedly toxic in animal models or possessed undesirable pharmacokinetic profiles. In addition, none of these agents were evaluated for antitumor or immunostimulatory effects.[4,6,8,9]

CD38 is already a validated target for cancer immunotherapy, since it is highly expressed on the surface of a variety of tumor cells, most notably multiple myeloma (MM). The monoclonal antibodies (MABs) daratumumab and isatuximab specifically bind to CD38 on the surface of these tumor cells and promote tumor cell death by Fc-dependent immune effector mechanisms including complement-dependent cytotoxicity (CDC), antibody-dependent cell-mediated cytotoxicity (ADCC), antibody-dependent cellular phagocytosis (ADCP), and

[a]*Dept. of Drug Discovery and Biomedical Sciences, Medical University of South Carolina, 70 President St, Charleston, SC 29425, USA. E-mail: woster@musc.edu*

[b]*Dept of Cell and Molecular Pharmacology and Experimental Therapeutics, Medical University of South Carolina, 173 Ashley Ave., Charleston, SC 29425, USA*

[c]*Dept of Pediatrics and Human Development, College of Human Medicine, Michigan State University, 400 Monroe Ave. NW, Grand Rapids, MI 49503, USA*

† Electronic supplementary information (ESI) available: Detailed experimental procedures, spectral data for synthesized intermediates. See DOI: 10.1039/d1ra06266b

apoptosis upon secondary cross-linking.[10–12] Because CD38 is also highly expressed on the surface of regulatory T-cells (Tregs), regulatory B-cells and myeloid suppressor cells, these MABs also reduce the number of immune suppressors, resulting in an increase in cytotoxic T-cells.[13,14]

Ironically, resistance to CD38-targeted MABs is mediated by CD38 itself. Importantly, CD38 up regulation appears to be one of the most important factors in mediating resistance to checkpoint blockade in MM and other cancers.[15–17] *In vitro* and *in vivo* studies demonstrate that CD38 inhibits $CD8^+$ T-cell function *via* adenosine (ADO) receptor signalling. In addition, resistance to PD-1/PD-L1 blocking antibodies is mediated through upregulation of CD38 and subsequent production of ADO.[15] Extracellular ADO binds to ADO receptors on immune cells, including T cells, natural killer (NK) cells, neutrophils, macrophages and dendritic cells, preventing their activation.[18,19] ADO produced by CD38 also promotes myeloid-derived suppressor cell (MDSC) expansion, macrophage M2 polarization, and $CD4^+$ Treg generation, all of which support tumor cell progression.[20] Taken together, these data indicate that CD38 or ADO receptor blockade are effective strategies to overcome this resistance.[21]

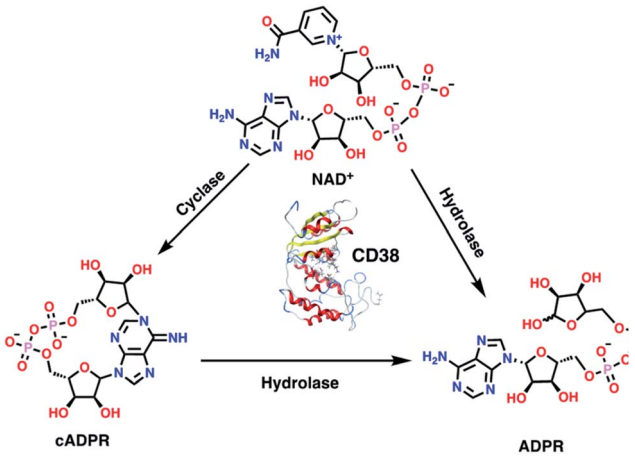

Fig. 1 Using two distinct catalytic reactions, CD38 produces ADP-ribose (ADPR) from both NAD^+ and cADPR.

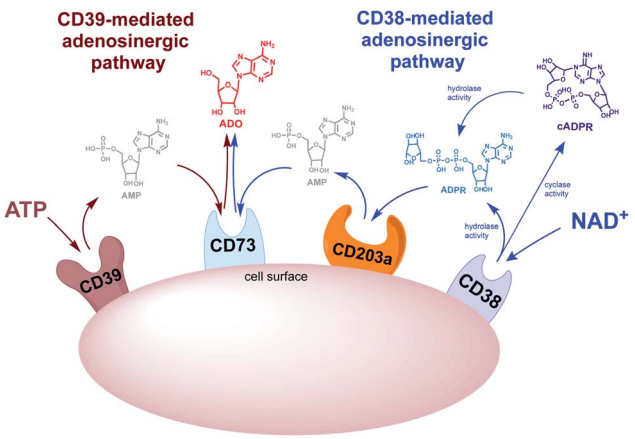

Fig. 2 CD38- and CD39-mediated adenosinergic pathways.

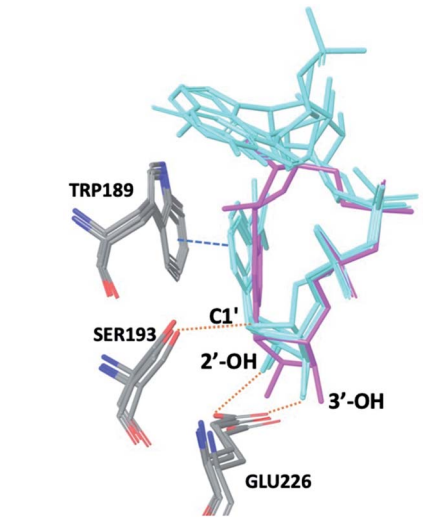

Fig. 3 Superimposition of PDB codes 2I65, 2O3S, 2O3U, and 4F45 displaying a consensus catalytic site and substrate orientation (NAD^+, NGD, cADPr (magenta), and NAADP). The nicotinamide ribose retains a conserved binding pose with substrates: NAD^+, NGD^+, and NAADP displayed in cyan. Purine location is solvent exposed and tends to lack a consensus binding position. In each structure TRP189, SER193, and GLU226 are responsible for forming critical contracts and mediate catalysis of each substrate. For clarity only the heavy atoms are shown, dotted orange lines represent hydrogen bonds, blue dashed line represent $\pi-\pi$ interactions.

Role of CD38 in cellular energy metabolism

As an ectoenzyme, CD38 plays a critical role in the homeostatic regulation of cellular energetics.[4,5] By metabolizing the cofactor NAD^+, CD38 removes an essential electron acceptor, thus limiting the energetic capacity of a cell. CD38 is known for its

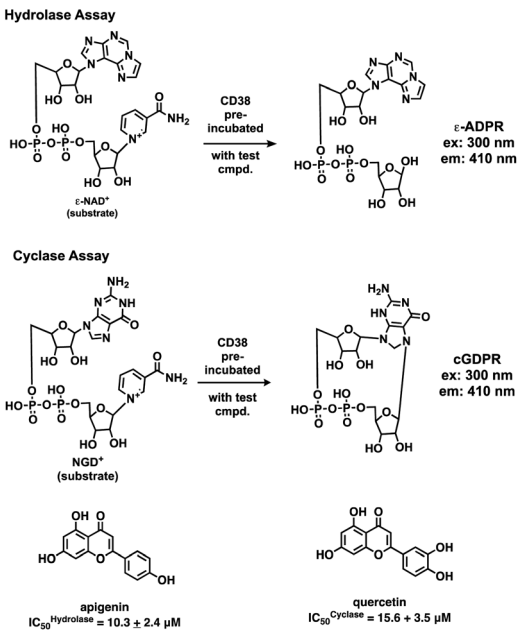

Fig. 4 Reactions comprising the CD38 hydrolase (top) and cyclase (bottom) assays, and structures of the standard inhibitors apigenin and quercitin.

Table 1 Structures of CD38 inhibitors and their activity against CD38 hydrolase and cyclase. *ND = not determined

Compound	Structure	M_W	% hydrolase activity remaining (50 μM)	% cyclase activity remaining (50 μM)	IC_{50} hydrolase (μM)	IC_{50} cyclase (μM)
1	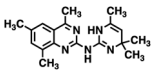	309.42	22.7 ± 0.40	60.9 ± 2.2	4.0 ± 0.48	>100 μM
2	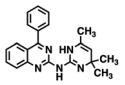	343.43	48.5 ± 2.3	57.0 ± 4.0	23.0 ± 1.0	ND*
3	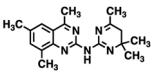	309.42	47.9 ± 1.2	52.1 ± 8.6	10.8 ± 0.7	ND*
4	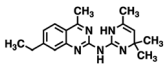	309.42	50.7 ± 1.7	48.0 ± 7.3	22.0 ± 1.0	ND*
5	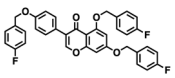	594.59	49.0 ± 1.5	40.0 ± 1.2	ND*	ND*
6	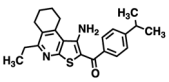	378.53	51.2 ± 4.8	28.1 ± 9.2	ND*	36.3 ± 8.6
7	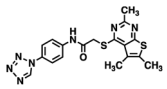	411.50	52.7 ± 6.1	53.9 ± 49.7	ND*	ND*
8	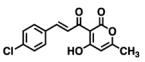	290.70	87.3 ± 0.3	17.1 ± 1.7	ND*	15.0 ± 3.9
9	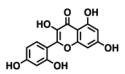	302.24	87.2 ± 3.4	21.0 ± 2.3	>100 μM	35.4 ± 7.6
10	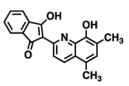	317.34	ND*	35.0 ± 4.1	ND*	5.2 ± 1.0
11	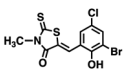	364.66	103 ± 2.2	19.3 ± 11.2	ND*	Insoluble
12	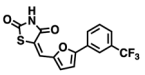	333.29	80.9 ± 4.4	12.9 ± 4.3	>100 μM	20.8 ± 4.0
13	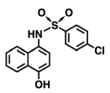	333.79	95.9 ± 1.4	24.0 ± 3.3	ND*	37.5 ± 18.6
14	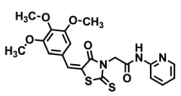	445.51	80.7 ± 3.7	−1.7 ± 10.3	ND*	16.6 ± 0.2
15	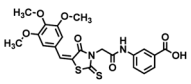	488.53	98.0 ± 3.9	38.4 ± 25	ND*	17.1 ± 4.3
16	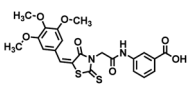	392.83	0.7 ± 0.4	23.1 ± 10.6	25.0 ± 3.0	23.4 ± 6.9
17 (50 nM)	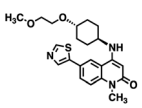	413.54	60.3 ± 1.8	95.7 ± 6.1	0.076 + 3.2	>1.0 μM

glycohydrolytic activity, though in some circumstances it uses two reactions that may be sequentially coupled (Fig. 1). In the first reaction, CD38 functions as a cyclase, removing nicotinamide from NAD^+ and producing cyclic adenosine diphosphate-ribose (cADPR).[4,22] CD38 also mediates an energetically more favorable hydrolase reaction that produces

adenosine diphosphate-ribose (ADPR) from both NAD^+ and cADPR.[1,4] CD38 over expression in immune cells and tumor cells within the tumor microenvironment (TME) causes a reduction in NAD^+ levels, leading to a down regulation of the immune response against tumor cells.[3] CD38-knockout $CD4^+$ T cells more effectively control tumor growth when compared to wild type $CD4^+$ T cells, express twice the level of interferon-gamma (IFNγ), and up regulate Sirt1,[23,24] a key NAD-dependent regulator of effector function within T cells.[24]

Role of CD38 in ADO generation

There are two adenosinergic pathways (Fig. 2) associated with exogenous adenosine (ADO) generation. The better-known pathway involves the nucleoside triphosphate diphosphohydrolase known as cluster of differentiation 39 (CD39). CD39 performs two sequential hydrolysis reactions: ADO triphosphate (ATP) is converted to ADO diphosphate (ADP) followed by the conversion of ADP to ADO monophosphate (AMP). Finally, the hydrolysis of AMP to ADO is mediated by the ectoenzyme cluster of differentiation 73 (CD73).[25] While the CD39 pathway has been regarded as the predominant source of exogenous ADO, there is skepticism regarding the complete functionality of this pathway *in vivo*. The optimal pH for CD39-mediated hydrolysis of ATP and ADP is 8.0–8.5, suggesting that ADO production *via* CD38 ADO may predominate in the acidic TME.[26–28] A lesser known adenosinergic pathway is mediated by CD38, which hydrolyzes NAD^+ to ADPR. ADPR is in turn converted to ADO by the ectoenzymes cluster of differentiation 203a (CD203a) and CD73 (Fig. 2).[29] Extracellular ADO, which is prominent in the TME, stimulates the ADO receptor, A2AR, on the surface of immune effector cells.[30,31] Collectively these transformations cause a shift from an ATP-driven proinflammatory environment to an anti-inflammatory milieu induced by ADO-mediated down regulation of immune function.[32,33]

Results and discussion

The observations above led us to initiate a screen for small molecule inhibitors of CD38 that are selective for either the cyclase or hydrolase activity of CD38 and to optimize their immunostimulatory activity through structural modification. In order to identify novel non-NAD^+ mimetic scaffolds as CD38 inhibitors, we constructed a model consensus structure of CD38 *via in silico* analysis of published substrate/inhibitor co-crystals of CD38 (PDB 2I65, 2O3U, 4F45, 4XJT and 2O3T) using the Molecular Operating Environment software (Chemical Computing Group, Montreal, CA) (Fig. 3).[34–38] After preparing each crystal structure at pH 7.4 and 310 K (see ESI for a complete description†), structures were superimposed to generate a consensus model of the CD38 active site. The model was then used to confirm the importance of GLU226 for catalysis *via* its ability to H-bond with 2′ and 3′ –OH of the nicotinamide-ribose. Furthermore, SER193 in the model structure of CD38 was observed proximal to the C1′ of the nicotinamide-ribose and has been implicated in the reaction

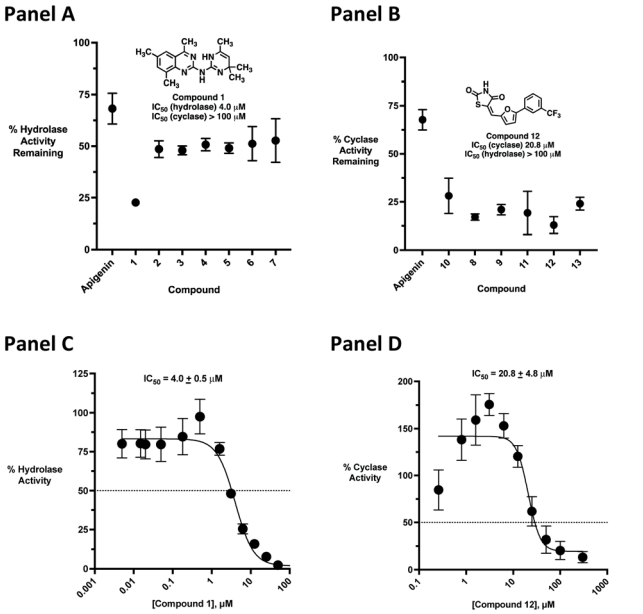

Fig. 5 Comparison of CD38 hydrolase- and cyclase-selective inhibitors at 50 μM. Panel A: top 7 hydrolase-selective inhibitors; panel B: top 7 cyclase-selective inhibitors; panel C: IC_{50} determination for compound **1** against CD38 hydrolase; panel D: IC_{50} determination for compound **12** against CD38 cyclase. All data points are the result of at least 3 determinations + SEM.

mechanism for NAD^+ degradation. The orientation of nicotinamide was mediated through aromatic interactions with TRP189. In both the original X-ray structure 4XJT and the generated model structure, phosphate groups were found stabilizing the complex and active site that were not involved with catalysis. However, despite ligand diversity across substrates and inhibitors, a consistent active site conformation was observed for all ligands screened virtually in the model structure of CD38. This geometric orientation of the active site and the cyclic nature of cADPR suggested the evaluation of heterocycles and macrocycles. Additionally, to mimic substrate interactions with TRP189, SER193, GLU146 and GLU226, nicotinamide and purine bio-isosteres were investigated. Most notably, an emphasis was placed on non-biological bioisosteres with structures not mimicking NAD^+, since NAD^+ analogues

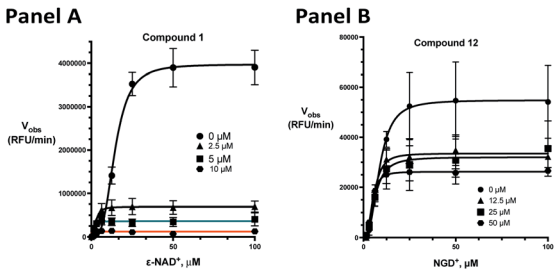

Fig. 6 Enzyme inhibition kinetics for the hydrolase and cyclase activities of CD38 by compounds **1** and **12**. Panel A: inhibition of CD38 hydrolase by compound **1**; panel B: inhibition of CD38 cyclase by compound **12**. All data points are the result of 3 determinations ± SEM.

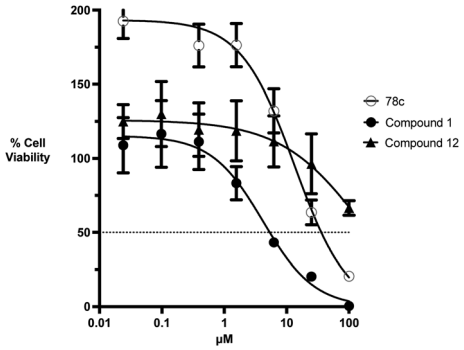

Fig. 7 Cytotoxicity of **78c**, **1** and **12** in naive PBMC cells at concentrations between 0.01 and 100 μM. All data points are the average of 9 determinations (3 donors each run in triplicate in separate experiments) ± SEM.

would have a greater potential for off-target effects at other NAD^+ binding sites. A curated compound library was then constructed consisting of compounds meeting the above criteria from the commercial Cambridge and Enamine drug screening compound sets, as well as previously synthesized compounds in our laboratory. A total of 100 compounds were selected for the initial *in silico* screen that included hemipeptidomimetic macrocycles, as well as mono-, bi-, and tricyclic heterocycles. We then used our consensus active site model to perform virtual screening of the curated library using standard docking experiments (Molecular Operating Environment, Montreal, CA). The 24 compounds with the most favorable docking scores were then selected and purchased for physical screening.

Initial screening was performed at a concentration of 50 μM of each compound in technical and experimental triplicates. Hydrolase or cyclase activities were monitored independently by using N^6-ethenonicotinamide adenine dinucleotide (ε-NAD^+) or nicotinamide guanine dinucleotide (NGD^+), respectively, as substrate, and monitoring fluorescence at 410 nm (Fig. 4).[39] The flavanoid apigenin, which has been shown to be an inhibitor of the hydrolase activity of CD38,[7] and quercitin, which has been shown to be an inhibitor of the cyclase activity of CD38,[7] were

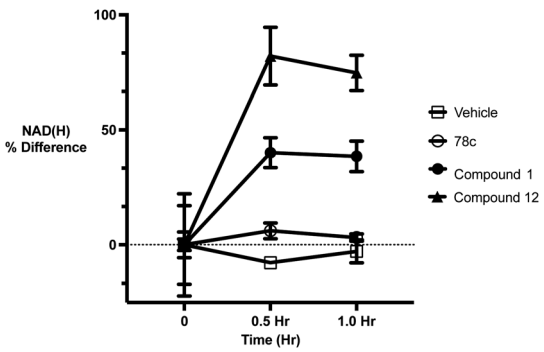

Fig. 8 Increases in cellular $NADH^+$ levels in activated PBMCs following treatment at 1 μM concentrations of **78c**, **1** and **12**. All data points are the average of 3 determinations ± SEM.

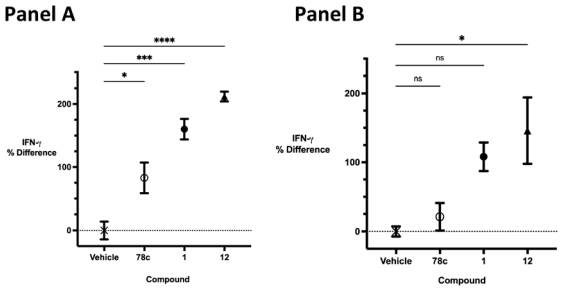

Fig. 9 Effect of **78c**, **1** and **12** at 10 μM on IFNγ levels. Panel A: 48 hours; panel B: 12 days.

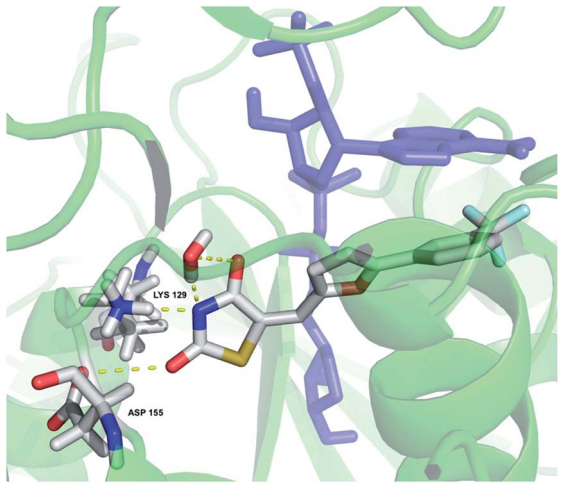

Fig. 10 *In silico* representation of compound **12** bound to the CD38 active site. Amino acids involved in binding and **12** are colored by atom type; the all-blue structure is NAD^+.

used as positive controls for the hydrolase and cyclase reaction, respectively. It should be noted that in our hands, neither compound showed significant selectivity for either activity, and both were significantly less potent than previously reported. Of the 24 selected compounds, 16 produced significant inhibition of CD38 (Table 1) and were then assayed for selectivity between the hydrolase and cyclase activities. Based on these data, compounds **1** (Fig. 5, panel A) and **12** (Fig. 5 panel B) were highly selective for their respective targets and were chosen for further study. Compound **1** exhibited an IC_{50} value of 4.0 μM against CD38 hydrolase (Fig. 5, panel C) and >100 μM against CD38 cyclase, while **12** had an IC_{50} of 20.8 μM against CD38 cyclase

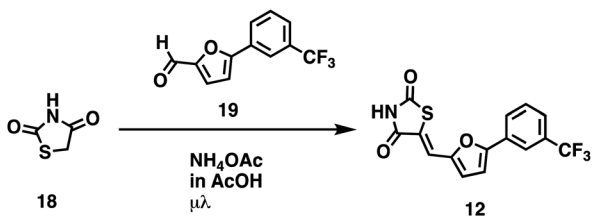

Scheme 1

Table 2 Structures of CD38 inhibitors and their activity against CD38 cyclase

Cmpd	Structure	M_W	% cyclase activity remaining (50 μM)	IC_{50} cyclase (μM)
20	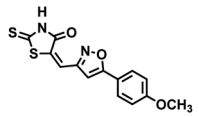	318.37	17.6 ± 2.1	3.71
21	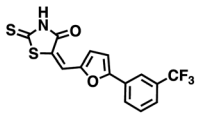	299.38	22.1 ± 4.0	11.53
22	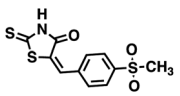	309.25	21.7 ± 8.1	4.81
23	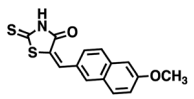	289.29	9.3 ± 0.8	4.65
24	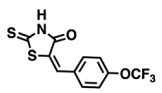	341.44	90.1 ± 3.9	>100
25	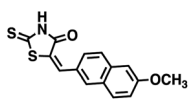	272.34	68.3 ± 18.2	56.0
26	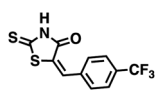	311.37	77.3 ± 22.4	>100
27	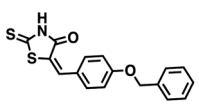	313.39	88.2 ± 0.6	>100
28	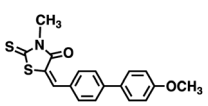	279.33	93.9 ± 6.9	>100
29	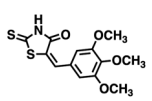	311.43	98.6 ± 4.7	>100
30	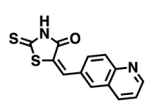	350.79	70.3 ± 40.7	20.9
31	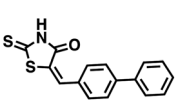	309.40	96.3 ± 6.8	>100
32	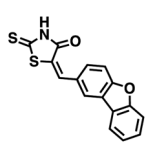	365.39	64.5 ± 4.2	3.15
33	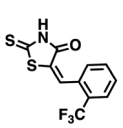	311.42	39.4 ± 4.9	10.0

Table 2 (*Contd.*)

Cmpd	Structure	M_W	% cyclase activity remaining (50 μM)	IC_{50} cyclase (μM)
34	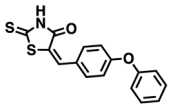	298.38	66.3 ± 23.4	56.0
35	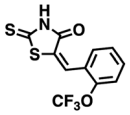	355.35	81.7 ± 9.0	>100
36	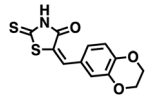	301.38	90.0 ± 5.4	>100
37	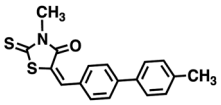	295.36	84.5 ± 2.2	>100
38	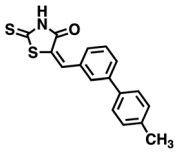	327.42	84.5 ± 8.5	>100
39	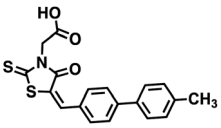	311.37	64.1 ± 7.2	68.6
40	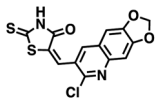	297.39	22.1 ± 14.3	43. 2
41	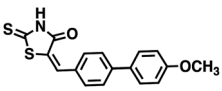	289.29	81.6 ± 2.4	>100
42	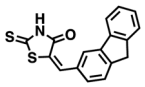	305.29	87.1 ± 3.4	>100
43	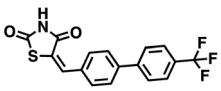	325.44	29.0 ± 18.8	48.2
44	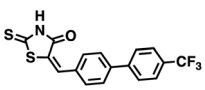	369.45	39.1 ± 2.7	35.0
45	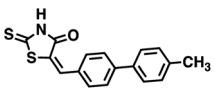	327.42	55.7 ± 2.3	53.8
46	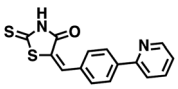	349.33	49.4 ± 27.1	42.7

(Fig. 5 panel D) and >100 μM against CD38 hydrolase. Compound **12** was selected for structural optimization primarily due to its selectivity for the CD38 cyclase activity and because it was the most synthetically feasible for library construction. Other compounds (*e.g.* **13** and **14**) will be elaborated in future studies.

The kinetic mechanism of inhibition for the hydrolase and cyclase activities of CD38 were determined using a standard Michaelis–Menten approach, as shown in Fig. 6. The results suggest that both **1** and **12** produce a mixed/uncompetitive inhibition of the hydrolase and cyclase activities, respectively. In our hands, the known inhibitor **78c** (**17**)[8,9] is a potent inhibitor of the hydrolase (IC_{50} 76 nM), but has very little activity against the cyclase. These data are consistent with the reported IC_{50} value for **17**, which exhibited an IC_{50} of 7 nM against CD38 hydrolase *via* mixed kinetics.[9] The difference in the IC_{50} value obtained in our laboratory is likely due to differences in assay conditions. The cytotoxicity of **1** was monitored in activated peripheral blood mononuclear cells (PBMCs) over a concentration range of 1 nM to 100 μM, as shown in Fig. 7. Compound **1** began to exhibit cytotoxic effects in PBMC cells at 1.0 μM, which is lower than its IC_{50} value. By contrast, compound **12** was relatively non-toxic up to 50 μM, which is 2.5-fold higher that its IC_{50} value.

To further demonstrate the effect of **1** and **12** on inhibition of CD38 and to monitor the biological efficacy of our hit molecules, increases in $NADH^+$ in activated PBMCs were monitored at 30 and 60 minutes after addition of the inhibitor. The known CD38 inhibitor **78c**[9] was used as a control. Compound **78c** had a modest effect on $NADH^+$ levels (Fig. 8), while **1** and **12** produced a 40.1 and 82.0% increase at 0.5 h, respectively. In both cases, elevated $NADH^+$ levels remained relatively stable at 1 h.

The effects of inhibitors **78c**, **1** and **12** on IFNγ levels was next examined after 48 hours and 12 days, as shown in Fig. 9. PBMCs were incubated with the appropriate inhibitor at 10 μM for the indicated time, and IFNγ levels were measured by ELISA. At 48 hours, compounds **1** and **12** produced 160.1 and 212.0% increases in IFNγ, respectively, compared to an 82.9% increase in IFNγ following treatment with **78c**. At 12 days, IFNγ levels were 21.1, 108.1 and 145.9% for **78c**, **1** and **12**, respectively, slightly lower than IFNγ levels observed after 48 hour incubation.

The binding mode of **12** in the CD38 active site was simulated starting with X-ray structure 4XJT, as shown in Fig. 10. The bound inhibitor 4-[(2,6-dimethylbenzyl)amino]-2-methylquinoline-8-carboxamide[8] and the covalent bond between ADPR and CD38 were removed, and compound **12** was docked in the active site as described above. In this model, the 2-thioxothiazolidin-4-one ring nitrogen appears to form hydrogen bonds with LYS 129 and ASP 155. In addition, the thiazolidine ring nitrogen and an adjacent carbonyl coordinate a water molecule in the active site. In this orientation, there appears to be a pi stacking arrangement between **12** and ADPR that stabilizes binding. This arrangement is consistent with the observed uncompetitive kinetics of inhibition since optimal binding depends on the presence of the substrate NAD^+. As the structure–activity relationships for binding of **12** and its analogues are further elucidated, the *in silico* model will be refined accordingly.

Library generation

We opted to produce a library of analogues of **12** due to their relative ease of synthesis compared to compound **1**. Compound

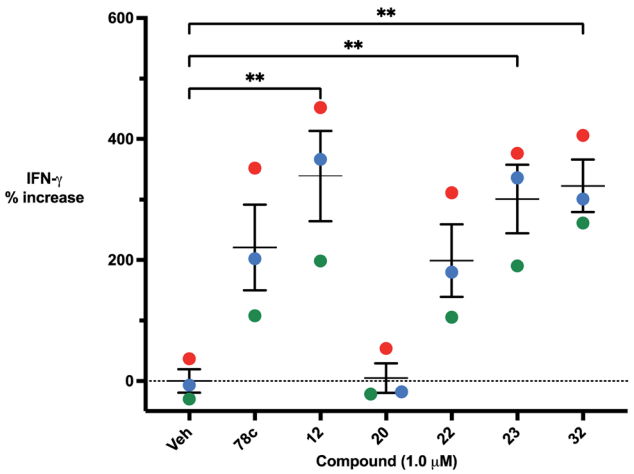

Fig. 11 48 hour increase in IFNγ in the presence of 1.0 μM compounds **78c**, **12**, **20**, **22**, **23** and **24** in activated PBMCs from three separate donors. Each data point is the average of 3 determinations (red = donor 1, blue = donor 2, green = donor 3). These averages were then replotted as % increase in IFNγ ± SEM.

12 could be synthesized in a single microwave step using a modified Knoevenagel condensation reaction between 2-thioxothiazolidin-4-one **18** and 5-(3-(trifluoromethyl)phenyl) furan-2-carbaldehyde **19** (Scheme 1) predominantly as the *Z*-isomer.[40–42] This synthetic approach was then employed to introduce chemical diversity during structural optimization, resulting in compounds **20–46** (Table 2).

Four of the compounds shown in Table 2 exhibited a lower IC_{50} against CD38 cyclase activity than **12** (compounds **20**, **22**, **23** and **32**). The ability of these compounds to increase IFNγ content in activated PBMCs from 3 separate donors was determined at 48 hours, as described above, and the results of these studies appear in Fig. 11. Compounds **12**, **23** and **32** were more effective than **78c** at increasing IFNγ, and the percent increase caused by compounds **22**, **23** and **32** was inversely proportional to their observed IC_{50} values. Among compounds **12**, **20**, **22**, **23** and **32**, compound **12** exhibited the greatest effect on IFNγ levels at 1.0 μM, despite having the highest IC_{50}. Because CD38 carries out its enzyme function both inside and outside the cell,[43] this finding may be due to an enhanced ability of **12** to penetrate into PBMCs.

Conclusions

A number of small molecule inhibitors of CD38 have been reported, but to date none have been evaluated for stimulatory effects in immune cells. We have identified a series of CD38 inhibitors based on a *Z*-5-ethylidinethiazolidine-2,4-dione scaffold that are potent inhibitors of CD38, and that in some cases show a marked selectivity for inhibition of cyclase activity. The most potent of these compounds, **32**, exhibits an IC_{50} value of 3.15 μM in the CD38 cyclase assay. We have further shown that these compounds inhibit CD38 by a mixed/uncompetitive mechanism. The parent molecule in this series, **12**, produced an 82% increase in NAD^+ content in naive PBMCs after 30

minutes, and a 212% increase in IFNγ levels after 48 hours that persisted for 12 days. Importantly, **12** was significantly more potent than the known CD38 inhibitor **78c** with regard to promoting increases in IFNγ. Compound **78c** was evaluated as an inhibitor of CD38 hydrolase, but not specifically as an inhibitor of CD38 cyclase. Since **12** and its analogues are cyclase-selective, our data suggests that the cyclase plays a greater role in activation of T-cell function than was previously thought.

With regard to structure–activity relationships (SAR), we have not made a sufficient number of analogues to make any meaningful statements concerning **12** and its analogues. However, the most active analogues (**12**, **20**, **22**, **23**, **30**, **32**) generally possess large phenyl or biphenyl substituents that are in conjugation with the Z-double bond moiety, and except for **20** are substituted with a halogen-containing substituent, indicating that binding to the cyclase catalytic site depends on π-interactions with nearby residues on the protein. We will refine our SAR model as additional active inhibitors become available. In addition, because these compounds have IC_{50} values in the micromolar range, the possibility of off-target effects exists. This issue will also be addressed in subsequent studies.

In this manuscript, we have described a number of cyclase-selective inhibitors of CD38 that will be of use in determining the role that the hydrolase and cyclase activities of CD38 play in metabolism, activation of immune cells and in the development of resistance to immune checkpoint inhibitors. It is not currently known whether the CD38 hydrolase or the CD38 cyclase activity makes the greatest contribution to down regulation of the immune response, or which activity contributes to the development of resistance to CD38 immune checkpoint inhibitors. Our data suggests that the CD38 cyclase plays a significant role on down regulation of the immune response and the development of resistance. We are now optimizing CD38 inhibitors that are structurally related to **1** to identify an inhibitor for use as a chemical probe for the hydrolase activity of CD38. With selective hydrolase and cyclase inhibitors as chemical tools, we will be able to determine to what extent selective inhibition of the hydrolase and cyclase activities of CD38 contribute to the activation of immune cells, and which activity plays the greatest role in development of resistance.

The critical role of CD38, which is expressed on B, NK and T-cells as well as macrophages, has been well studied as a target for cancer immunotherapy.[44–46] As mentioned above, CD38 metabolism has been shown to be a major factor in the development of resistance to MABs.[15–17,47] As such, the CD38 inhibitors described herein may be of great value as adjuncts to existing therapy with checkpoint inhibitors such as daratumumab and isatuximab. However, CD38 inhibition could also be exploited in the treatment of other diseases resulting from depletion of NAD^+ and/or over production of ADO. Decreases in NAD^+ levels are associated with various metabolic diseases (diabetes, obesity, dyslipidemia and nonalcoholic fatty liver)[48,49] and in aging.[50–52] It also plays a major role in the immune response to infectious disease[53] including COVID-19.[54] ADO is a potent immunosuppressant, and plays a similar role in the development and progression of disease.[54] Taken together, these observations indicate an increasing medical need for small molecule inhibitors of CD38 for use in diseases where dysregulated NAD^+ and ADO metabolism are a factor. For this reason, the optimization of the compounds described in this paper, as well as the discovery of additional scaffolds for CD38 inhibition, is an ongoing concern in our laboratories.

Author contributions

Thomas Z. Benton, conceptualization, data curation, formal analysis, methodology, writing - original draft; Catherine Mills, conceptualization, data curation, formal analysis, methodology, writing – original draft; Jonathan Turner, investigation, validation; Megan J. Francis, investigation; Dalan Soloman, investigation; Pieter B. Burger, formal analysis, methodology, software, visualization; Yuri Peterson, formal analysis, methodology, software, visualization; Nathan Dolloff, formal analysis, methodology; Andre Bachmann, formal analysis, methodology, review and editing; Patrick M. Woster, conceptualization, data curation, formal analysis, funding acquisition, project administration, resources, supervision, writing – original draft, review and editing.

Conflicts of interest

None of the authors of this manuscript have any conflicts to declare.

Acknowledgements

Completion of the experiments delineated in this manuscript were supported in part through participation of the MUSC Drug Discovery Core and the MUSC Nuclear Magnetic Resonance Core.

Notes and references

1 H. C. Lee, *Mol. Med.*, 2006, **12**, 317–323.
2 L. Fagerberg, B. M. Hallstrom, P. Oksvold, C. Kampf, D. Djureinovic, J. Odeberg, M. Habuka, S. Tahmasebpoor, A. Danielsson, K. Edlund, A. Asplund, E. Sjostedt, E. Lundberg, C. A. Szigyarto, M. Skogs, J. O. Takanen, H. Berling, H. Tegel, J. Mulder, P. Nilsson, J. M. Schwenk, C. Lindskog, F. Danielsson, A. Mardinoglu, A. Sivertsson, K. von Feilitzen, M. Forsberg, M. Zwahlen, I. Olsson, S. Navani, M. Huss, J. Nielsen, F. Ponten and M. Uhlen, *Mol. Cell. Proteomics*, 2014, **13**, 397–406.
3 G. Shubinsky and M. Schlesinger, *Immunity*, 1997, **7**, 315–324.
4 E. N. Chini, C. C. S. Chini, J. M. Espindola Netto, G. C. de Oliveira and W. van Schooten, *Trends Pharmacol. Sci.*, 2018, **39**, 424–436.
5 E. N. Chini, *Curr. Pharm. Des.*, 2009, **15**, 57–63.
6 M. Dong, Y. Q. Si, S. Y. Sun, X. P. Pu, Z. J. Yang, L. R. Zhang, L. H. Zhang, F. P. Leung, C. M. Lam, A. K. Kwong, J. Yue, Y. Zhou, I. A. Kriksunov, Q. Hao and H. C. Lee, *Org. Biomol. Chem.*, 2011, **9**, 3246–3257.

7 C. Escande, V. Nin, N. L. Price, V. Capellini, A. P. Gomes, M. T. Barbosa, L. O'Neil, T. A. White, D. A. Sinclair and E. N. Chini, *Diabetes*, 2013, **62**, 1084–1093.

8 J. D. Becherer, E. E. Boros, T. Y. Carpenter, D. J. Cowan, D. N. Deaton, C. D. Haffner, M. R. Jeune, I. W. Kaldor, J. C. Poole, F. Preugschat, T. R. Rheault, C. A. Schulte, B. G. Shearer, T. W. Shearer, L. M. Shewchuk, T. L. Smalley Jr, E. L. Stewart, J. D. Stuart and J. C. Ulrich, *J. Med. Chem.*, 2015, **58**, 7021–7056.

9 C. D. Haffner, J. D. Becherer, E. E. Boros, R. Cadilla, T. Carpenter, D. Cowan, D. N. Deaton, Y. Guo, W. Harrington, B. R. Henke, M. R. Jeune, I. Kaldor, N. Milliken, K. G. Petrov, F. Preugschat, C. Schulte, B. G. Shearer, T. Shearer, T. L. Smalley Jr, E. L. Stewart, J. D. Stuart and J. C. Ulrich, *J. Med. Chem.*, 2015, **58**, 3548–3571.

10 M. B. Overdijk, J. H. Jansen, M. Nederend, J. J. Lammerts van Bueren, R. W. Groen, P. W. Parren, J. H. Leusen and P. Boross, *J. Immunol.*, 2016, **197**, 807–813.

11 N. van de Donk, P. G. Richardson and F. Malavasi, *Blood*, 2018, **131**, 13–29.

12 N. W. van de Donk, M. L. Janmaat, T. Mutis, J. J. Lammerts van Bueren, T. Ahmadi, A. K. Sasser, H. M. Lokhorst and P. W. Parren, *Immunol. Rev.*, 2016, **270**, 95–112.

13 J. Krejcik, T. Casneuf, I. S. Nijhof, B. Verbist, J. Bald, T. Plesner, K. Syed, K. Liu, N. W. van de Donk, B. M. Weiss, T. Ahmadi, H. M. Lokhorst, T. Mutis and A. K. Sasser, *Blood*, 2016, **128**, 384–394.

14 N. van de Donk, *Immunol. Lett.*, 2018, **199**, 16–22.

15 L. Chen, L. Diao, Y. Yang, X. Yi, B. L. Rodriguez, Y. Li, P. A. Villalobos, T. Cascone, X. Liu, L. Tan, P. L. Lorenzi, A. Huang, Q. Zhao, D. Peng, J. J. Fradette, D. H. Peng, C. Ungewiss, J. Roybal, P. Tong, J. Oba, F. Skoulidis, W. Peng, B. W. Carter, C. M. Gay, Y. Fan, C. A. Class, J. Zhu, J. Rodriguez-Canales, M. Kawakami, L. A. Byers, S. E. Woodman, V. A. Papadimitrakopoulou, E. Dmitrovsky, J. Wang, S. E. Ullrich, Wistuba II, J. V. Heymach, F. X. Qin and D. L. Gibbons, *Cancer Discov.*, 2018, **8**, 1156–1175.

16 S. Koyama, E. A. Akbay, Y. Y. Li, G. S. Herter-Sprie, K. A. Buczkowski, W. G. Richards, L. Gandhi, A. J. Redig, S. J. Rodig, H. Asahina, R. E. Jones, M. M. Kulkarni, M. Kuraguchi, S. Palakurthi, P. E. Fecci, B. E. Johnson, P. A. Janne, J. A. Engelman, S. P. Gangadharan, D. B. Costa, G. J. Freeman, R. Bueno, F. S. Hodi, G. Dranoff, K. K. Wong and P. S. Hammerman, *Nat. Commun.*, 2016, **7**, 10501.

17 P. C. Tumeh, C. L. Harview, J. H. Yearley, I. P. Shintaku, E. J. Taylor, L. Robert, B. Chmielowski, M. Spasic, G. Henry, V. Ciobanu, A. N. West, M. Carmona, C. Kivork, E. Seja, G. Cherry, A. J. Gutierrez, T. R. Grogan, C. Mateus, G. Tomasic, J. A. Glaspy, R. O. Emerson, H. Robins, R. H. Pierce, D. A. Elashoff, C. Robert and A. Ribas, *Nature*, 2014, **515**, 568–571.

18 S. Goh, H. H. M. Ng, V. Chew, X. N. Sim, H. Li, S. Lim, J. C. T. Lim, J. J. H. Loh, K. Sabai, C. C. H. Ong, T. Loh, W. Q. Leow, J. L. J. Xin, H. C. Toh, F. Malavasi, D. W. M. Tai, S. Y. Lee, P. Chow, E. Newell, S. P. Choo, J. Yeong and T. K. H. Lim, *bioRxiv*, 2019, 638981, DOI: 10.1101/638981.

19 A. Passarelli, M. Tucci, F. Mannavola, C. Felici and F. Silvestris, *Tumour Biol.*, 2019, **42**(4), 1–10.

20 B. E. Kennedy, M. Sadek, M. O. Elnenaei, A. Reiman and S. A. Gujar, *Trends Cancer*, 2020, **6**, 9–12.

21 V. Quarona, G. Zaccarello, A. Chillemi, E. Brunetti, V. K. Singh, E. Ferrero, A. Funaro, A. L. Horenstein and F. Malavasi, *Cytometry, Part B*, 2013, **84**, 207–217.

22 P. F. Egea, H. Muller-Steffner, I. Kuhn, C. Cakir-Kiefer, N. J. Oppenheimer, R. M. Stroud, E. Kellenberger and F. Schuber, *PLoS One*, 2012, **7**, e34918.

23 S. Chatterjee, A. Daenthanasanmak, P. Chakraborty, M. W. Wyatt, P. Dhar, S. P. Selvam, J. Fu, J. Zhang, H. Nguyen, I. Kang, K. Toth, M. Al-Homrani, M. Husain, G. Beeson, L. Ball, K. Helke, S. Husain, E. Garrett-Mayer, G. Hardiman, M. Mehrotra, M. I. Nishimura, C. C. Beeson, M. G. Bupp, J. Wu, B. Ogretmen, C. M. Paulos, J. Rathmell, X. Z. Yu and S. Mehrotra, *Cell Metab.*, 2018, **27**, 85–100.

24 M. R. Fernandez and J. L. Cleveland, *Cell Metab.*, 2018, **27**, 3–5.

25 G. G. Yegutkin, T. Henttinen, S. S. Samburski, J. Spychala and S. Jalkanen, *Biochem. J.*, 2002, **367**, 121–128.

26 D. B. Leal, C. A. Streher, T. N. Neu, F. P. Bittencourt, C. A. Leal, J. E. da Silva, V. M. Morsch and M. R. Schetinger, *Biochim. Biophys. Acta*, 2005, **1721**, 9–15.

27 M. Milosevic, S. Petrovic, N. Velickovic, I. Grkovic, M. Ignjatovic and A. Horvat, *Mol. Cell. Biochem.*, 2012, **371**, 199–208.

28 E. L. Gordon, J. D. Pearson and L. L. Slakey, *J. Biol. Chem.*, 1986, **261**, 15496–15507.

29 A. L. Horenstein, A. Chillemi, G. Zaccarello, S. Bruzzone, V. Quarona, A. Zito, S. Serra and F. Malavasi, *Oncoimmunology*, 2013, **2**, e26246.

30 J. Blay, T. D. White and D. W. Hoskin, *Cancer Res.*, 1997, **57**, 2602–2605.

31 *Tumor-induced immune suppression: mechanisms and therapeutic reversal*, ed. D. I. Gabrilovich and A. A. Hurwitz, Springer, 2nd edn, 2014, pp. 411–434.

32 L. Antonioli, P. Pacher, E. S. Vizi and G. Hasko, *Trends Mol. Med.*, 2013, **19**, 355–367.

33 A. L. Horenstein, C. Bracci, F. Morandi and F. Malavasi, *Front. Immunol.*, 2019, **10**, 760.

34 R. Graeff, Q. Liu, I. A. Kriksunov, Q. Hao and H. C. Lee, *J. Biol. Chem.*, 2006, **281**, 28951–28957.

35 R. Graeff, Q. Liu, I. A. Kriksunov, M. Kotaka, N. Oppenheimer, Q. Hao and H. C. Lee, *J. Biol. Chem.*, 2009, **284**, 27629–27636.

36 Q. Liu, I. A. Kriksunov, R. Graeff, H. C. Lee and Q. Hao, *J. Biol. Chem.*, 2007, **282**, 5853–5861.

37 Q. Liu, I. A. Kriksunov, R. Graeff, C. Munshi, H. C. Lee and Q. Hao, *Structure*, 2005, **13**, 1331–1339.

38 Q. Liu, I. A. Kriksunov, R. Graeff, C. Munshi, H. C. Lee and Q. Hao, *J. Biol. Chem.*, 2006, **281**, 32861–32869.

39 J. Camacho-Perreira, M. G. Tarrago, C. C. S. Chini, C. Escande, G. M. Warner, A. S. Puranik, R. A. Schoon,

J. M. Reid, A. Galina and E. N. Chini, *Cell Metab.*, 2016, **23**, 1127–1139.
40 K. A. Kandeel, *Chem. Pap.*, 2004, **58**, 334–340.
41 A. J. Russell, I. M. Westwood, M. H. Crawford, J. Robinson, A. Kawamura, C. Redfield, N. Laurieri, E. D. Lowe, S. G. Davies and E. Sim, *Bioorg. Med. Chem.*, 2009, **17**, 905–918.
42 Y. Song, D. T. Connor, R. Doubleday, R. J. Sorenson, A. D. Sercel, P. C. Unangst, B. D. Roth, R. B. Gilbertsen, K. Chan, D. J. Schrier, A. Guglietta, D. A. Bornemeier and R. D. Dyer, *J. Med. Chem.*, 1999, **42**, 1151–1160.
43 H. C. Lee and Y. J. Zhao, *J. Biol. Chem.*, 2019, **294**, 19831–19843.
44 L. Gao, Y. Liu, X. Du, S. Ma, M. Ge, H. Tang, C. Han, X. Zhao, Y. Liu, Y. Shao, Z. Wu, L. Zhang, F. Meng and F. Xiao-Feng Qin, *Cell Death Dis.*, 2021, **12**, 680.
45 F. Morandi, A. L. Horenstein, F. Costa, N. Giuliani, V. Pistoia and F. Malavasi, *Front. Immunol.*, 2018, **9**, 2722.
46 F. Morandi, A. L. Horenstein and F. Malavasi, *Front. Immunol.*, 2021, **12**, 658263.
47 F. M. Uckun, *Cancers*, 2021, **13**, 2018–2031.
48 D. J. Li, S. J. Sun, J. T. Fu, S. X. Ouyang, Q. J. Zhao, L. Su, Q. X. Ji, D. Y. Sun, J. H. Zhu, G. Y. Zhang, J. W. Ma, X. T. Lan, Y. Zhao, J. Tong, G. Q. Li, F. M. Shen and P. Wang, *Theranostics*, 2021, **11**, 4381–4402.
49 K. Okabe, K. Yaku, K. Tobe and T. Nakagawa, *J. Biomed. Sci.*, 2019, **26**, 34.
50 R. Zapata-Perez, R. J. A. Wanders, C. D. M. van Karnebeek and R. H. Houtkooper, *EMBO Mol. Med.*, 2021, **13**, e13943.
51 H. Massudi, R. Grant, N. Braidy, J. Guest, B. Farnsworth and G. J. Guillemin, *PLoS One*, 2012, **7**, e42357.
52 X. H. Zhu, M. Lu, B. Y. Lee, K. Ugurbil and W. Chen, *Proc. Natl. Acad. Sci. U.S.A.*, 2015, **112**, 2876–2881.
53 B. Groth, P. Venkatakrishnan and S. J. Lin, *Front. Mol. Biosci.*, 2021, **8**, 686412.
54 N. J. Habeichi, C. Tannous, A. Yabluchanskiy, R. Altara, M. Mericskay, G. W. Booz and F. A. Zouein, *Int. Rev. Immunol.*, 2021, 1–11.